

THE DEVELOPMENT OF A QUICK SCREEN IN YEAST FOR FUNCTIONAL
EPITHELIAL SODIUM CHANNELS

Presented to the Graduate Council of
Texas State University-San Marcos
in Partial Fulfillment
of the Requirements

for the Degree

Master of SCIENCE

by

Raquel V. Ybanez, B.S.

San Marcos, Texas
August 2009

ACKNOWLEDGEMENTS

I would like to thank all people who have supported and inspired me over the last two years. I especially want to thank my advisor, Dr. Rachell Booth, for all of her guidance during my research and study at Texas State. Her advice, encouragement, and patience made this project possible. I will always be grateful for her mentorship in training me to be a better scientist. I would also like to thank my committee members Dr. Kevin Lewis and Dr. Wendi David. I am especially appreciative of the time they took to offer insight and suggestions when I needed it the most. Dr. Lewis deserves special mention because not only did he donate all of the yeast strains, but he also offered much insight into working with yeast in general. I would also like to acknowledge Jim Stockand at the UT Health Science center at San Antonio for contributing the samples of mutated alpha ENaC for me to work with. They were an integral part of this project and I greatly appreciated this kind donation. Additionally, I would like to thank the entire Chemistry & Biochemistry faculty and staff at Texas State for creating a learning environment where I could not only learn, but also excel. I always appreciated how everyone was so willing to teach and support all students that walked through their doors. I will always look back fondly on the time I spent here.

I would also like to express my gratitude to my lab partners; their company and support made long hours in the lab just fly by. I would like to especially thank Jenny Browning and Daniel Sauls for always being so supportive and willing to lend a helping hand. I have truly enjoyed working with you both. Additionally, I would like to thank

former lab members, Lyndsey Kirk and Mikki Boswell, who both made contributions to the ENaC project and thus aided me in my work, and Candice Gonzales who taught me how to do the cloning required for this project.

Lastly, I would like to thank Justin Duhon. Words cannot express how much your love, support, and encouragement has meant to me. Thank you for the late dinners, the cancelled plans, and the trips to San Marcos with me on weekends and nights; I know you thought trips to the lab at midnight were crazy, but I loved your company. Lastly, your willingness to do this for five more years and travel half way across the country as I continue to pursue my training as a scientist astounds me and I can't believe how lucky I am to have found someone like you. Thank you so very much for being the person who enables my dreams.

This manuscript was submitted on July 13, 2009.

TABLE OF CONTENTS

	Page
ACKNOWLEDGEMENTS	iii
LIST OF TABLES	vi
LIST OF FIGURES	vii
ABSTRACT.....	ix
CHAPTER	
I. INTRODUCTION AND LITERATURE REVIEW	1
II. MATERIALS AND METHODS.....	13
III. RESEARCH RESULTS AND DISCUSSION	24
IV. CONCLUSIONS.....	48
REFERENCES	51

LIST OF TABLES

Table	Page
1: Custom primers used in PCR.....	16
2: List of restriction enzymes used to digest samples.....	17
3: List of sequencing primers.....	18
4: Strains of <i>S. cerevisiae</i> used in the expression of ENaC	19
5: Summary of mutant alpha ENaC functions	20
6: Summary of deletion strains used in the alpha ENaC screen	45

LIST OF FIGURES

Figure	Page
1: Schematic of a distal tubule kidney epithelial cell	2
2: General depiction of ENaC/DEG family topology and homology.....	4
3: ENaC is inhibited by amiloride	5
4: Predicted heterotrimeric structure of human ENaC.....	6
5: Scheme for ENaC regulation	9
6: PCR amplification and digestion of the alpha ENaC gene.....	26
7: Vector map of pYES2NT	27
8: Digestion of pYES2NT DNA	28
9: Screen for correctly ligated pYES2NT-alpha ENaC	30
10: Vector map of pYES2NT-alpha ENaC.....	31
11: Western blot of alpha ENaC expression in <i>S. cerevisiae</i>	33
12: Dilution pronging to assay salt sensitivity.....	34
13: Growth curves to assay salt sensitivity.	35
14: Immunocytochemistry of <i>S. cerevisiae</i> expressing alpha ENaC	36
15: Dilution pronging to assay amiloride rescue	37
16: The effects of amiloride on growth.....	39

17: Screen for correctly ligated pYES2NT-His1-alpha ENaC	40
18: Dilution pronging assay of alpha ENaC mutants.....	41
19: Western blot of alpha ENaC mutants.	43
20: Dilution pronging assay of deletion strains	46

ABSTRACT

THE DEVELOPMENT OF A QUICK SCREEN IN YEAST FOR FUNCTIONAL EPITHELIAL SODIUM CHANNELS

by

Raquel V. Ybanez

Texas State University-San Marcos

August 2009

SUPERVISING PROFESSOR: RACHELL E. BOOTH

Epithelial sodium channels (ENaC) are voltage independent Na^+ channels found in the lining of the lungs, salivary glands, and kidneys. Situated within the apical membrane of epithelial cells, ENaC works in conjunction with a Na^+/K^+ ATPase to transport Na^+ through the cell. In water permeable cells the movement of Na^+ triggers the movement of water through the cell as well. This function is especially critical in the distal portion of the kidney tubule where Na^+ and water must be reabsorbed in order to maintain appropriate blood pressure levels (1). Anomalous ENaC activity can lead to

disorders such as Liddle's syndrome, which is due to overactive ENaC and is characterized by severe hypertension, or pseudohypoaldosteronism type I, which is caused by decreased ENaC activity and results in hypotension (2).

Understanding the structure of ENaC as it relates to function is essential to understanding ENaC's physiological role. We report development of an expression system in yeast that allows us to quickly screen the level of activity for various ENaC mutants. The screen takes advantage of ENaC's ability to transport Na^+ into the cell and cause growth inhibition (3). Yeast cells expressing wild type ENaC display a salt sensitivity phenotype when grown on high salt media, but cells expressing an ENaC mutant that is no longer functional do not. These results can easily be visually compared through the use of a survival pronging dilution assay. This will allow for future identification of loss of function mutants, which can then be further examined to determine exactly how and why they are critical for function.

Additionally, viability for utilizing the assay to screen strains from the *Saccharomyces* Genome Deletion Project was also examined. We report the identification of four genes required for proper ENaC function in yeast: *SUR4*, *ERV14*, *EMP24*, and *ERV25*.

CHAPTER I

INTRODUCTION AND LITERATURE REVIEW

Sodium is the most osmotically active cation circulating in the extracellular fluid, and all higher organisms must regulate its concentration in order to maintain sodium homeostasis. In humans, decreased sodium levels lead to dehydration and metabolic acidosis, while elevated levels can cause high blood pressure and strain on the circulatory and renal systems (1-3). Therefore, it is paramount that regulatory mechanisms are in place to ensure that the amount of sodium absorption can be adjusted so that dietary intake equals loss through excretion. In this delicate balance, epithelial sodium channels (ENaC) play a vital role, as they are responsible for the fine tuning of sodium absorption in tissues such as the distal kidney, colon, and lung epithelia.

ENaCs are voltage independent sodium channels situated within the apical membrane of tight junction epithelial cells. They are known for being constitutively active, highly selective for sodium and lithium ions over potassium, and especially sensitive to channel inactivation by the diuretic amiloride. ENaC's physiological role is most important in the kidney and the colon where sodium transport is crucial for the maintenance of blood sodium levels and whole body homeostasis. In the lungs and salivary glands, sodium transport is not critical to whole body homeostasis, but rather it is needed for keeping the composition and the volume of the luminal fluid constant.

To achieve vectorial transport of sodium through the cell, ENaC works in conjunction with a Na^+/K^+ ATPase on the basolateral membrane (Figure 1). The Na^+/K^+ ATPase provides the driving force for this process by using the energy of adenosine triphosphate (ATP) to actively pump sodium into the blood. This creates a depletion of sodium in the cell and allows sodium to passively travel down its electrochemical gradient through ENaC. This classifies ENaC as a passive transporter. The movement of sodium into the cell affects the osmolarity of the intracellular fluid causing water to passively move through channels termed aquaporins demonstrating the close relationship between sodium concentration and water balance (4).

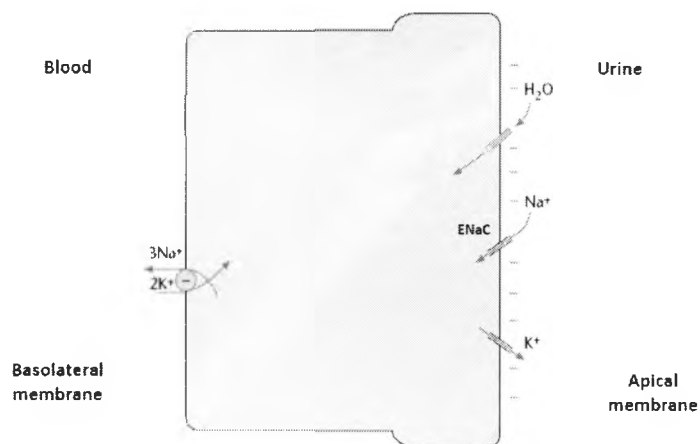


Figure 1: Schematic of a distal tubule kidney epithelial cell. In this scenario, sodium travels from the urine into the cell via an open ENaC. Once inside the cell, sodium is actively pumped out by a Na^+/K^+ ATPase into the blood. The net result is sodium reabsorption within the kidney nephron. ENaC activity is the primary limiting factor for sodium reabsorption in these epithelia (5).

ENaC is a heterotrimeric channel composed of three homologous subunits termed α , β , and γ . Each subunit contributes to ion channel formation and each is required for maximal ENaC activity. These subunits are approximately 650-700 amino acids in length

sharing approximately 30% amino acid sequence identity to one another (6). ENaC subunits are not splice variants from a single gene, but are encoded by three separate genes, SCNN1A, SCNN1B, and SCNN1G, which mostly likely arose from a single ancestor gene. Gene orthologs are also well conserved, with 60% homology from *Xenopus laevis* to man and about 85% homology for rat to man (7,8).

The structural features of ENaC classify it as a member of the ENaC/degenerin (ENaC/DEG) ion channel superfamily, which includes degenerins (DEG) and acid-sensing ion channels (ASIC). Members of the DEG/ENaC superfamily have been examined in a variety of organisms including nematodes, amphibians, flies, humans, and found in tissues such as kidney epithelia, muscle, and neurons. Family members show a diverse range of biological functions including salt regulation, mechanosensation, sensory perception, and pain sensation. To accomplish this wide range of tasks these sodium channels exhibit a wide range of gating properties. Some channels, like ENaC, are not ligand gated but are constitutively active, while others are ligand gated, like ASICs which are activated upon the binding of a proton. While gating mechanisms may vary, the topology of all family members is invariant. Structural features include two transmembrane regions, a relatively large and cysteine-rich extracellular loop that may be glycosylated at several points, and relatively short cytosolic tails (Figure 2A). More than one-half of the channel forms the extracellular loop, which is a structural feature not found in other ion channel families. Additionally all members share conserved regions, such as the pre-membrane spanning domain (MDS) 1 region, which is implicated in gating, despite various mechanisms by which members may actually be gated, and the

pre-MSD2 loop, which is thought to contribute to channel pore formation (8) (Figure 2B).

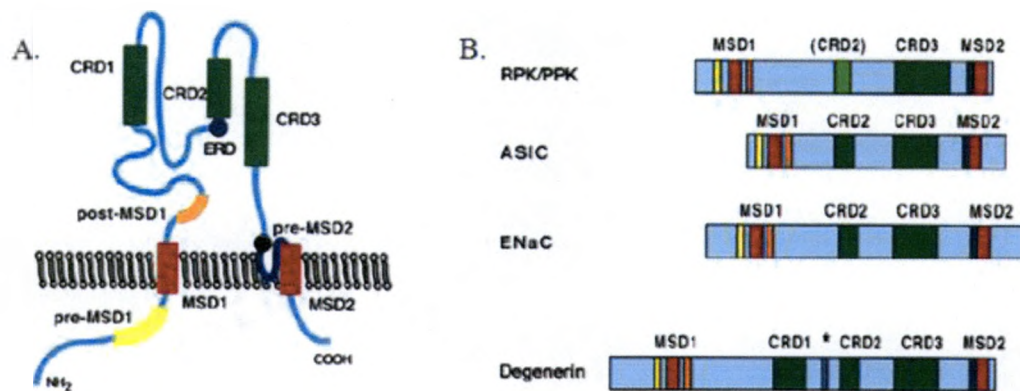


Figure 2: General depiction of ENaC/DEG family topology and homology. (A) The general topology of an individual ENaC/degnerin subunit. The largest part of the protein is situated outside the cell, while both termini are located in the intracellular cytoplasm. Conserved regions are labeled, such as membrane spanning domains (MSD) and cysteine rich domains (CRD). (B) Homologous regions are compared between ENaC/degnerin superfamily members. Note that CRD1 and extracellular regulating domain (ERD) are unique to degnerins; CRD3 is the most conserved domain, while CRD2 is only partially conserved across subfamilies (8,9).

Another feature that is shared by all ENaC/degnerins members is the presence of a highly conserved amino acid sequence known to code for the amiloride binding site (Figure 3). ENaC is unique among channels in this family due to its high affinity for amiloride, as ENaC experiences channel block at submicromolar levels of amiloride. Amiloride is a pore blocker and competitive inhibitor of sodium. The reason that ENaC is much more sensitive to amiloride may lie in the presence of a Ser residue at position α S583; other family members contain a glycine at this site and show lower affinities for amiloride. Kellenberger *et al.* showed that when the substitution α S583G is made the result is decreased affinity for amiloride by ENaC (10). Additionally, it mattered little

whether the mutation was to Cys, Ala, or Asp, suggesting that altered backbone torsion angles accessible only to Gly are responsible for this loss of affinity (11). They concluded that the Ser-Gly-Ser-Gly arrangement of ENaC's amiloride binding site may in part account for its high affinity for amiloride. However, it should be noted that amiloride block is complex, likely involves other residues, and still remains to be fully resolved.

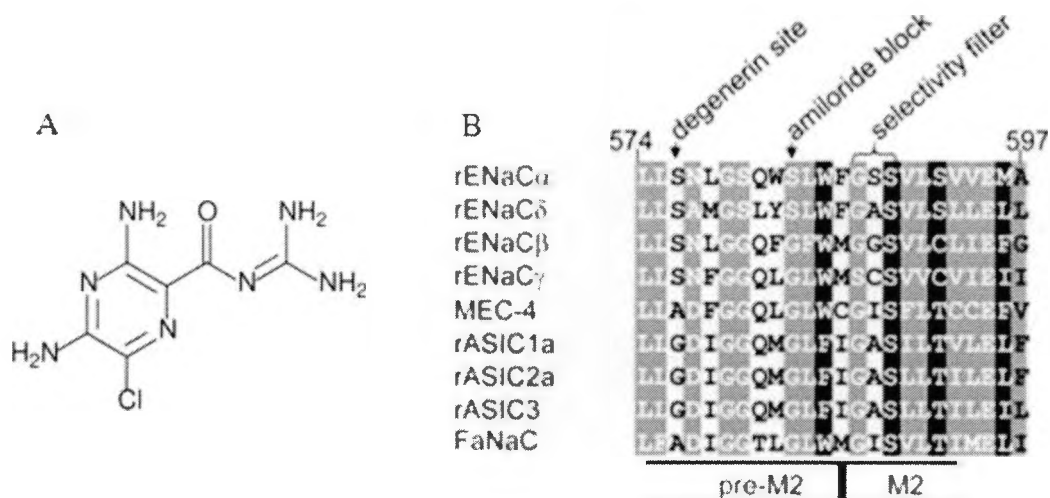


Figure 3: ENaC is inhibited by amiloride. The structure of amiloride is shown in (A), while an alignment of the ENaC pore region is shown in (B). The pre-membrane spanning segment (pre-M2) and the N-terminal part of M2 which make up the outer pore entry and selectivity filter of ENaC are shown. Black shading indicates 100% conserved and gray shading indicates 80% or greater conserved. Note that the serine at the amiloride block position in rat alpha ENaC (as well as delta) differs from all others including the beta and gamma ENaC subunits. (10).

Currently the structure of ENaC has not been elucidated. The challenge in generating a crystal structure has been primarily due to the low levels at which ENaC is expressed and the difficulty in purification of sufficient quantities for X-ray crystallography. The best structure of ENaC available is a model based on the structure of another ENaC/degenerin member, chicken ASIC (cASIC), which was solved by Jasti *et al.* (Figure 4) (7,12). cASIC, a neuronal acid-sensing ENaC/DEG channel, shares

approximately 20% amino acid sequence homology with ENaC. A comparison of the two shows that heterotrimeric ENaC, as well as individual ENaC subunits within the trimer, share a great deal of secondary, tertiary, and quaternary features with cASIC. However, subtle differences between the two may explain the different gating mechanisms, as well as ENaC's insensitivity to acid. For example, ENaC subunits do not have any of the 13 cASIC1 residues implicated directly in proton binding. Additionally, ENaC lacks a tryptophan homologous to cASIC1 Trp288, which is suggested to play a role in channel activation or inactivation following proton binding. This may explain why ENaC is constitutively open, rather than proton gated.

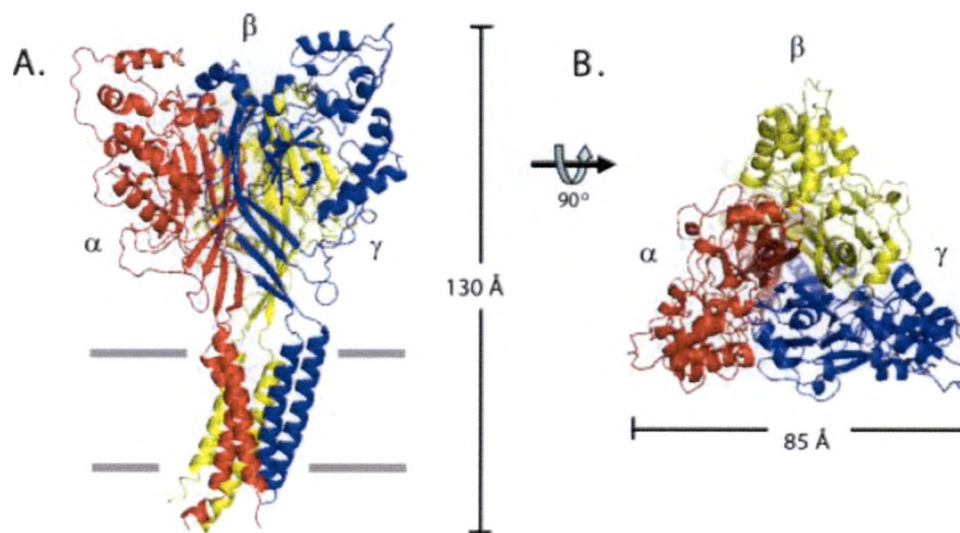


Figure 4: Predicted heterotrimeric structure of human ENaC. Many scientists believe that ENaC stoichiometry is 1:1:1 in accordance with cASIC subunit stoichiometry revealed by its crystal structure. The ribbon structure is shown in (A) parallel and (B) perpendicular from the extracellular side. Alpha is red, beta is yellow, and gamma is blue (7).

ENaC subunits prefer to orient in an equal ratio as a heterotrimeric channel rather than homomeric channels. For many years scientists debated over the preferred stoichiometry in which the subunits associated, but new experimental evidence suggests that the preferred stoichiometry of the channel is $1\alpha:1\beta:1\gamma$. One such experiment was conducted by Staruschenko *et al.* using total internal reflection fluorescence (TIRF) microscopy to measure plasma membrane fluorescence signals in simian kidney (COS) cells. Each subunit was labeled with a fluorophore and the signal intensity was compared between the subunits. This study found that when α , β , and γ are co-expressed subunit composition is fixed in a $1\alpha:1\beta:1\gamma$ ratio (13). In light of this evidence and the close fit between homotrimeric cASIC1 and heterotrimeric hENaC, it is likely that there is $1\alpha:1\beta:1\gamma$ stoichiometry of ENaC's subunits.

Alternative stoichiometries of ENaC subunits can also form *in vivo*. Randrianarison *et al.* demonstrated this in a study that examined fluid clearance in newborn mice with a disruption in the β ENaC gene (14). This disruption resulted in the up-regulation of α and γ ENaC, but overall function of the channel was only slightly impaired. It is widely accepted that $\alpha\beta$, $\alpha\gamma$, and α only can form functional ENaC channels at the surface of the cell membrane, but that these combinations have diminished activity and decreased stability when compared to the heterotrimeric channel (15). $\beta\gamma$ channels have also been observed, however they are located in the intracellular fluid rather than the membrane, suggesting that they may only represent channel precursors (16).

ENaC subunits are synthesized, modified, and packaged in the endoplasmic reticulum (ER) before being trafficked together to the cell surface. An important event

that occurs in this processing of all three ENaC subunits is the addition of the post-translational modification, N-linked glycosylation, on sites located on the extracellular domain. Glycosylation allows interactions with ER folding chaperones like calnexin or calreticulin, for recognition by quality control mannosidase-like proteins prior to exit from the ER, and for general stabilization of the folded state which protects the protein core from protease digestion (17).

The expression of ENaC at the cell surface is the prime determinant in regulating the amount of sodium actually absorbed. When sodium levels are low and renal absorption needs to be increased, aldosterone and vasopressin are released, stimulating the expression of more ENaC channels at the apical (lumen) surface of the cell (Figure 5). Aldosterone stimulates ENaC function by increasing the synthesis of ENaC channels. The mechanism for aldosterone action on ENaC primarily occurs due to an increase in transcription of the ENaC subunits, but aldosterone may also indirectly activate ENaC by interaction with other proteins, such as serum- and glucocorticoid-induced protein kinases (SGK). SGK inhibits channel degradation and thus stimulates ENaC simply by increasing channel half-life. Vasopressin modulates ENaC by binding to receptors on the basolateral membrane, which activates adenylate cyclase and results in an increase in cAMP levels. ENaC responds to increased cAMP by up-regulating channel exocytosis thus sending more ENaC to the cell surface.

ENaC expression must also be able to be decreased in response to high levels of sodium in the blood. Again this is primarily accomplished by modifying the number of channels at the surface of the cell, as opposed to altering the channel gating (18). The protein, Nedd4, decreases the number of ENaC channels at the surface by labeling ENaC

for degradation by ubiquitination (Figure 5). Ubiquitination is a process by which ubiquitin is added to a protein; this post-translational modification then serves as a signal to the cell to degrade the protein. In the case of ENaC, the subunits must be polyubiquitinated before they are excised from the membrane and degraded. Additionally, ENaC inhibition can also occur due to increased cytosolic sodium, providing negative feedback regulation.

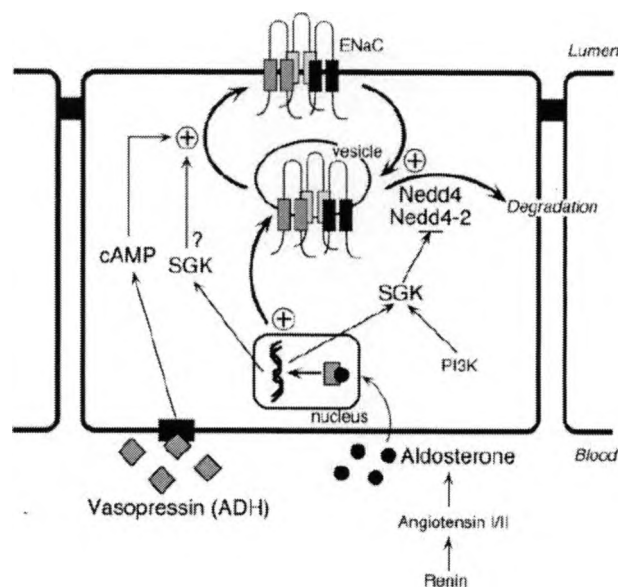


Figure 5: Scheme for ENaC regulation. The primary determinant for cell surface regulation is the result of ENaC insertion and degradation. Aldosterone and vasopressin stimulate channel synthesis, while Nedd4 modulates exocytosis of channels (18).

While membrane insertion and retrieval have long been thought to be the primary mechanisms for ENaC regulation, there is also evidence that proteolysis may be another means of regulation. Research by Vallet, V. *et al.* suggests that a low level of extracellular trypsin may increase channel activity, and conversely that extracellular serine protease inhibitors, such as aprotinin and bikunin, can decrease channel activity

(19). Other proteases, such as furin, prostatic, channel activating protease (CAP2), matriptase, kallikrein and elastase have also been shown to activate ENaC by cleaving channel subunits at defined sites within their extracellular domains (20). Proteases likely indirectly activate ENaC as well by cleaving and activating other proteases that subsequently cleave the channel. One example, prostatic, is translated as a proenzyme that must be cleaved to be active, but is not active until cleaved by matriptase (CAP3) (21). While it is evident that ENaC is activated by proteases by enhancing channel open probability, the mechanism on how cleavage modulates ENaC remains to be elucidated.

Two disease states have been linked to ENaC dysregulation. The first, Liddle's syndrome, is characterized by an activating mutation that results in an increase in sodium absorption. This is primarily due to a mutation which prevents ENaC from being ubiquitinated thus increasing channel presence at the membrane. Clinically, patients with Liddle's syndrome present with hypertension, low aldosterone, and low rennin (22). At the other extreme is the inactivating mutation of ENaC known as Pseudohyperaldosteronism I, which is characterized by a decrease in sodium absorption due to a mutation that renders ENaC incapable of responding to aldosterone (23). The kidneys are not able to reabsorb the sodium the body requires to function normally resulting in hypotension, salt wasting, and high aldosterone. These two disorders demonstrate that ENaC plays a critical role of blood pressure control and hypertension for individuals with genetic mutations to ENaC. Due to the complex nature of ENaC regulation, there may be a vast number of other mutations that may contribute to blood pressure irregularities in otherwise normal individuals.

Understanding the structure of ENaC as it relates to function is essential to understanding ENaC's physiological role, regulation, and pathophysiology. The goal of this project was to develop an expression system using *Saccharomyces cerevisiae* that would allow the level of activity for various ENaC mutants to be quickly screened. The screen would take advantage of ENaC's ability to transport sodium into the cell and cause growth inhibition (24). Yeast cells expressing wild type ENaC should display a salt sensitivity phenotype when grown on high salt media, but cells expressing an ENaC mutant that is no longer functional should not. The use of a survival pronging dilution assay could then be used to visually compare growth inhibition. The development of this screen would allow for the identification of structural motifs and residues critical to proper ENaC function. Once loss of function mutants are identified, these mutations can then be further examined to determine exactly how and why they are critical for function.

The screen could also be used to identify cellular proteins that play a role in ENaC expression. By utilizing the screen with the *Saccharomyces* Genome Deletion Project, which is a library of yeast strains that each lack one nonessential gene or "knockouts", genes critical to ENaC expression could be identified (25). This could be helpful in identifying human homologs of these critical genes, thus identifying potential targets for ENaC regulation. Furthermore, there is supporting evidence that a yeast screen for ENaC function can be developed. Gupta and Canessa have already reported expressing functional alpha and beta subunits in *S. cerevisiae* and that these cells were salt sensitive (26). Hass *et al.* reported success in developing a screen for function for the inwardly rectifying potassium (Kir) channel and using this screen with strains from the

Saccharomyces Genome Deletion Project to identify proteins necessary for ion channel function (27).

Development of the screens and the information they provide certainly refine our understanding of ENaC function and regulation. We hope that such studies will lead toward the identification of critical structural elements, as well as genes important for proper ENaC function.

CHAPTER II

MATERIALS AND METHODS

The reagents used to make all media: Luria-Bertani (LB) broth, tryptone, agar, yeast extract and yeast nitrogen base were from Becton Dickinson (Sparks, MD). All other reagents were purchased from Sigma-Aldrich (St. Louis, MO) unless otherwise noted. Reagents and materials were sterilized in an AS12 Autosterilizer from VWR Scientific (West Chester, PA). Microscale centrifugation was performed on a Beckman Coulter Microfuge 18 centrifuge (Fullerton, CA), while macroscale centrifugation was carried out on a Beckman Coulter J2-21 centrifuge. All equipment used to make and run the agarose gels was purchased from Invitrogen (Carlsbad, California) with the exception of the agarose, which was purchased from Shelton Scientific (Shelton, CT). All equipment used to make and run the polyacrylamide gels was purchased from Bio-Rad (Hercules, CA). Fermentas (Glen Burnie, Maryland) PageRuler™ Prestained Protein Ladder with 10 prestained recombinant prokaryotic proteins covering molecular weights from 10 to 170 kDa was used as a molecular weight standard. All gel images were acquired with a Kodak 440CF Digital Science Image Station (Eastman Kodak, New Haven, CT).

Transformation of plasmid DNA into *Escherichia coli*

Competent Top10 *E. coli* cells were transformed with the plasmid DNA of interest. The cells were thawed on ice for 20 min, 50-100 ng of plasmid DNA was added to 100 μ L cells, and the mixture was incubated on ice for an additional 10 min. The mixture was then heat shocked by placement in a 42 °C heat block for 45 seconds. At this point 1 mL of LB broth was added and the cells were incubated with shaking at 37 °C for 1 hour. Then 50 μ L was plated onto LB plates containing 100 μ g/mL ampicillin and grown overnight at 37 °C.

Isolation of plasmid DNA

A single colony was inoculated and grown overnight at 37° C in 5 mL of LB supplemented with 100 μ g/mL ampicillin. All plasmids were isolated from Top10 *E. coli* cells using a Qiagen QIAprep Spin Miniprep kit (Valencia, CA) following the manufacturer's protocol. The protocol called for the use of lysis and neutralization solutions, as well as a column to purify the plasmid DNA. Confirmation of plasmid isolation was determined by horizontal gel electrophoresis; plasmid concentrations were measured by placing 2 μ L of plasmid DNA in a Nanodrop ND-1000 Spectrophotometer from Thermo Fisher Scientific (Wilmington, DE).

Horizontal gel electrophoresis

A 50 mL, 1.0% (w/v) agarose gel in 1X TAE Buffer (40 mM Tris-base, pH 8, 20 mM acetic acid, 1 mM EDTA) was prepared and loaded with a 1 μ L sample of DNA

(unless otherwise noted) mixed with 1 μL 10X Endorstop (10 mM EDTA, 5 % v/v glycerol, 0.1 % w/v SDS, 0.01 % w/v bromophenol blue, pH 8.0) and enough ddH₂O to bring the total volume to 10 μL . The DNA samples were loaded into the gel and separated by electrophoresis for 60 min at 100 volts. The gel was then stained with a dilute ethidium bromide solution (0.2 mg EtBr/ml) for 20 min, rinsed with water, and imaged.

Polymerase chain reaction (PCR)

The PCR reactions included 100 ng of template DNA, 1 μM custom primers from IDT Integrated DNA Technologies, Inc (Coralville, IA) (Table 1), 0.4 mM dNTPs from Stratagene (La Jolla, CA), 1X ThermoPol buffer from New England Biolabs (NEB) (Ipswich, MA), and 0.1 units NEB Vent polymerase (New England Biolabs) in a total volume of 50 μL . The reactions were carried out in an Applied Biosystems 2720 Thermo Cycler (Foster City, CA) under the following run conditions: 94 °C for 2 min; twenty-five cycles of 94 °C for 30 seconds, 45 °C for 30 seconds, 72 °C for 2 min; 72 °C for 10 min; 4 °C for infinity. Once the PCR reaction was complete, 5 μL of the reaction mixture was analyzed with horizontal gel electrophoresis. PCR product cleanup was performed on the rest of the reaction mixture (approximately 45 μL) using a Promega Wizard PCR Preps DNA Purification System (Madison, WI) following the protocol provided. This protocol required using a membrane binding solution to bind the sample to the column, several washes with the wash solution provided, and elution with water.

Table 1: Custom primers used in PCR.

Primer Name	Primer Sequence
Alpha ENaC Forward (EcoRI)	5' GCAAGAATTCTTATGCTGGACCACACCAGAGCCCC 3'
Alpha ENaC Reverse (NotI)	5' GCAAGCGGCCGCTCAGAGTGCCATGGCCGGAGC 3'

Digestion

In separate reactions, the PCR product and cloning vector were prepared for ligation using restriction enzyme digestion. The reaction mixture included 450 ng of DNA, 10 units of restriction enzyme, and the appropriate NEB buffer at a 1X final concentration. Digestion reactions were carried out for two hours at 37 °C. Reactions containing the PCR products were stopped with 1X Endorstop. Alternatively, reactions containing the vector, pYES2NT-A (Invitrogen), were stopped by incubating the reaction at 65 °C for 20 min followed by the addition of 20 units of NEB Calf Intestinal Phosphatase (CIP). The use of CIP required an additional incubation at 37 °C for 1 hour; the reaction was stopped with 1X Endorstop. Horizontal gel electrophoresis was performed on all digestion products. The digestion product bands were extracted and cleaned using Promega Wizard PCR Preps DNA Purification System (Madison, WI) following the protocol provided. This protocol required incubating the gel bands with membrane binding solution at 60 °C and then centrifugation of the samples in the column provided. Several washes with the wash solution provided were done and then the digestion products were eluted in water.

Table 2: List of restriction enzymes used to digest samples.

Plasmid Name	Enzyme 1	Enzyme 2	NEB Buffer
Alpha ENaC PCR	EcoRI	NotI	EcoRI Buffer
pYES2NT-A	EcoRI	NotI	EcoRI Buffer

Ligation

Alpha ENaC was ligated into pYES2NT-A by adding the two together in a 3:1 ratio. The ligation reaction contained 150 ng of digested PCR product, 50 ng of digested vector DNA, 1X T4 DNA ligase buffer (NEB), and 400 units T4 DNA ligase (NEB). A control reaction of vector DNA only was also set up to determine the efficiency at which the vector could re-ligate with itself. All reactions were incubated at room temperature for 15 min. Next 10-20 μ L of the ligation reaction was transformed into chemically competent Top10 *E. coli* cells and plated on LB plates containing 100 μ g/ml ampicillin. Colonies containing the insert and vector were isolated, plasmid DNA was purified, and sent for sequencing.

DNA Sequencing

A 400-500 ng/mL sample of isolated plasmid DNA in water and 3 μ M of custom primers were sent to Davis Sequencing (Table 3). The sequences were checked for mutations by comparison to known sequences.

Table 3: List of sequencing primers.

Primer Name	Primer Sequence
<i>GALI</i> Forward	5' AATATACCTCTATACTTTAACGTC 3'
Alpha Internal	5' ACAACTCTTCCTACACTCGC 3'
V5 Reverse	5' ACCGAGGAGAGGGTTAGGGAT 3'

Transformation of plasmid DNA into *Saccharomyces cerevisiae*

Alpha ENaC in pYES2NT-A was transformed into *S. cerevisiae* cells using the following protocol (See Table 4 for strains used). A 1.0 mL culture of YPDA broth (1% w/v yeast extract, 2% w/v peptone, 0.02% adenine, and 2% w/v glucose) was inoculated with *S. cerevisiae* cells until the broth became cloudy; the solution was added to 4.0 mL of YPDA broth and incubated for 16 hours at 30 °C with shaking. After 16 hours, the entire cell culture was centrifuged at $6,000 \times g$ for five min. The supernatant was removed and the cells were resuspended in 1.0 mL of sterile ddH₂O. Once again the cells were centrifuged at $6,000 \times g$ for five min. The cells were then resuspended in 0.5 mL of 0.1 M lithium acetate, centrifuged at $14,000 \times g$ for thirty seconds, and then the supernatant was removed. Then 240 μ L of 50 % w/v polyethylene glycol 4000, 36 μ L of 1 M lithium acetate, 5 μ L of 10 mg/mL sonicated salmon sperm DNA (Stratagene), 65 μ L of H₂O, and 5 μ L of the plasmid DNA (≥ 100 ng/ μ L) were added to the cells. The samples were vortexed and then placed into the 30 °C shaker for 15-30 min. The tubes were immediately transferred to a 42 °C water bath for 20 min and then centrifuged for 30 seconds at $14,000 \times g$ to pellet the cells. The supernatant was removed and the cells were re-suspended in 200 μ L of water. After re-suspension, the cells were plated on selective synthetic media (2% w/v glucose, 0.67% w/v yeast nitrogen base, 0.01% w/v of

leucine and tryptophan, 0.005% w/v histidine, 0.14 v% w/v yeast drop out media, 2% w/v agar, and 0.5% w/v ammonium sulfate). Alpha ENaC in pYES2NT was plated on glucose minus uracil media because it has a *URA3* gene on the plasmid for selection.

Table 4: Strains of *S. cerevisiae* used in the expression of ENaC.

Strain	Genotype
BY4742	<i>MATα his3Δ1 leu2Δ lys2Δ ura3Δ</i> (28)
S1InsE4A	<i>MATα ura3-52 leu2-3,112 trp1-289 his7-2 ade5-1 lys2::InsE-4A</i> (29)

ENaC expression in *S. cerevisiae*

Yeast colonies were patched out onto selective media plates containing 2% w/v glucose and incubated for 2-3 days at 30 °C. Cells were then collected from the plate and placed into 10 mL of selective media containing 2% w/v raffinose and grown in a 30 °C shaker overnight. The OD₆₀₀ was measured and the amount required to inoculate a 25 mL culture so that the OD₆₀₀ = 0.4 was determined. This amount of cultured media was centrifuged at 1500 × g for 5 min and the supernatant was discarded. The cells were then washed with 1 mL of ddH₂O and once again centrifuged at 1500 × g for 5 min. The cells were then re-suspended in 1 mL of selective media containing 2% w/v galactose and then transferred into 25 mL of induction media which were placed in the 30 °C shaker. After 6 hours had elapsed, the OD₆₀₀ was measured and the entire culture was centrifuged at 1500 × g for 5 min, the supernatant was discarded, and the cell pellet was stored at -20 °C

To verify expression the cell pellets were thawed on ice and re-suspended in 500 μ L of breaking buffer (50 mM Na₃PO₄, 1 mM PMSF, and 5% glycerol). The resuspended pellet was centrifuged at 1500 × g for 5 min to re-pellet the cells. The

supernatant was once again removed and the cells were re-suspended in a volume of breaking buffer to obtain an $OD_{600} = 200$. An equal volume of acid washed beads was added to the mixture and the cells were subjected to 4 cycles of 30 seconds of vortexing followed by 30 seconds on ice. The cells were then centrifuged at $18,000 \times g$ for 10 min and the supernatant was collected.

BCA (bicinchoninic acid) protein assay

The BCA Protein Assay kit (Pierce) was used to determine the total protein concentration of the cell lysate. Samples being assayed were diluted 1/10 in ddH₂O and compared to bovine serum albumin (BSA) standards of known concentrations. The BCA reagents used were 50 parts BCA reagent A to 1 part reagent B. 200 μ L of the BCA reagent mixture was incubated with 10 μ L of standard or sample at 37 °C for 30 min. The absorbance was measured at 562 nm using a SpectraMax 190 plate reader with Softmax Pro 4.7.1 software and a standard curve was created using Microsoft Excel. The best-fit line from the standard curve was used to calculate the concentration of total protein in the lysate.

Sodium dodecyl sulfate polyacrylamide gel electrophoresis (SDS-PAGE)

For SDS-PAGE, 200 μ g of the whole cell lysate was mixed with 5X SDS Buffer (10% (v/v) glycerol, 62.5 mM Tris-HCl, pH 6.8, 2% (w/v) SDS, 0.0025% (w/v) bromophenol blue, 5% (v/v) β -mercaptoethanol), heated at 95 °C for five min, and loaded onto a 4% stacking gel (30 % v/v bis-acrylamide, 0.5 M Tris-HCl, pH 6.8, 10 % v/v SDS, 0.1 % v/v TEMED, and 10% w/v ammonium persulfate) and a 7.5% resolving gel (30 %

v/v bis-acrylamide, 1.5 M Tris-HCl pH 8.8, 10 % v/v SDS, 0.05 % v/v TEMED, and 10 % w/v ammonium persulfate). Separation by electrophoresis was carried out at 150 volts for 1.0 hours in 1X Running buffer (25 mM Tris-base, 1.9 M glycine, and 0.1 % v/v SDS, pH 8).

Western blot analysis

After electrophoresis the gel was placed in a blotting module with a nitrocellulose membrane. The blotting apparatus was filled with transfer buffer (1X Tris-glycine, 20% methanol) and an ice block was inserted into the apparatus. The blot was transferred for 45 min at a constant 100 volts. The nitrocellulose membrane was removed and washed in blocking solution (5% w/v milk, 150 mM NaCl, 10 mM Tris, 0.1% v/v Tween-20, pH 7.5 for 30 min. A 1/5000 dilution of anti-Xpress antibody [mouse] (Invitrogen) in blocking solution was added and incubated at 4 °C overnight. The nitrocellulose membrane was then washed three times with TBST (150 mM NaCl, 10 mM Tris, 0.1% v/v Tween-20, pH 7.5). A 1/20,000 dilution of horseradish peroxidase (HRP) conjugated anti-mouse antibody [rabbit] (Kirkegaard & Perry Laboratories) in blocking solution was added and incubated for 1 hour with agitation. The blot was washed two times with TBST and one time with TBS-no Tween for five min each. Detecting the HRP activity required adding 0.5 mL each of a two part Western Lighting kit (Perkin Elmer LAS, Inc.) solution to the blot for 1 min. The excess solution was discarded. The blot was exposed to X-ray film (ThermoFisher) for 1 to 10 min and then placed into a film developer.

Dilution pronging survival assays

Cells were harvested into 1 mL sterile ddH₂O. An aliquot of the stock was diluted 1/40, sonicated for 10 seconds at 1-5 watts using a Sonics Vibracell Ultrasonic Processor (Newtown, CT), and quantitated using a Reichert hemocytometer (Buffalo, NY) on a Comcon LOMO phase contrast microscope. Yeast cells were added to a sterile 96 well plate to achieve a concentration of 1×10^7 cells per 220 μ L. Cells were serially diluted 5-fold across the length of the plate. The cells were then pronged onto selective synthetic media containing galactose to induce expression of ENaC. Pronged plates were then incubated at 30 °C for 3-6 days and images of the cells were taken using a Samsung L100 digital camera (Ridgefield Park, NJ).

Growth curve assays

Yeast cells were patched out onto selective media plates containing 2% w/v glucose and incubated for 2-3 days at 30 °C. Cells were then collected from the plate and placed into 5 mL of selective media containing 2 % w/v glucose, the additional salt when appropriate, and grown in the 30 °C shaker overnight for 16-20 hours. The next day the culture media was changed to 10 mL of synthetic media containing 2% w/v raffinose, the additional salt when appropriate, and grown another 16-20 hours. The OD₆₀₀ was measured and the amount required to inoculate a 25 mL culture so that the OD₆₀₀ = 0.4 was calculated. This volume of cells was used to inoculate 25 mL of synthetic media containing 2% w/v galactose and the additional salt when appropriate. An initial OD₆₀₀ was measured (0 hour) before the cultures were placed in the incubator at 30 °C with

shaking. Growth curves were constructed by measuring the absorbance at 600 nm every 2 h for 8 hours followed by a reading at 24 hours.

Amiloride rescue test

Yeast cells were patched out onto selective media plates containing 2 % w/v glucose and incubated for 2-3 days at 30 °C. Cells were then collected from the plate and placed into 5 mL of selective media containing 2 % w/v glucose, the additional salt when appropriate, and grown in the 30 °C shaker overnight for 16-20 hours. The next day the culture media was changed to 10 mL of synthetic media containing 2% w/v raffinose, the additional salt when appropriate, and grown another 16-20 hours. The OD₆₀₀ was measured and the amount required to inoculate a 25 mL culture so that the OD₆₀₀ = 0.4 was calculated. This volume of cells was used to inoculate 25 mL of synthetic media containing 2% w/v galactose, the additional salt where appropriate, and the amiloride in the concentration being examined. An initial OD₆₀₀ was measured (0 hour) before the cultures were placed in the incubator at 30 °C with shaking. After 24 hours of growth, the final OD₆₀₀ was recorded.

CHAPTER III

RESEARCH RESULTS AND DISCUSSION

In an effort to identify critical amino acids within the alpha ENaC subunit, we aimed to develop a quick screen for ENaC function in yeast. This first required creating an expression system that would result in functional alpha ENaC within the membrane of yeast cells. Previous experiments had attempted expression of a C-terminal 6x histidine tagged alpha ENaC, but this construct did not result in functional ENaC channel expression in yeast despite the fact that mammalian expression systems have utilized detection and purification tags on the C-terminal region without apparent loss in function (30). Therefore to achieve expression of functional alpha ENaC channels in yeast, the first goal of this project was to sub-clone and express an N-terminal 6x histidine tagged alpha ENaC and verify its functionality.

Functionality of the expressed alpha ENaC was assessed with a standard yeast dilution pronging survival assay, which demonstrated that *S. cerevisiae* cells transformed with the plasmid pYES2NT-Alpha ENaC were salt sensitive. Next, we aimed to determine whether a dilution pronging survival assay could be utilized to distinguish between mutants of alpha ENaC. Five mutants of alpha ENaC with various levels of activity were also sub-cloned into pYES2NT and examined with the dilution pronging survival assay. Our results demonstrated various levels

of salt sensitivity indicating that when expressed in yeast, survival pronging can be used to detect variations in ENaC mutant function.

Amplification of the Alpha ENaC Gene

The initial goal was to create a new plasmid containing the alpha ENaC gene under the control of the regulatable *GALI* promoter and with an N-terminal 6x histidine tag. In order to prepare the alpha ENaC gene for ligation into the digested pYES2/NT vector, the murine alpha ENaC gene from a pCMV-Myc vector was first PCR amplified with Vent polymerase. This required custom forward and reverse primers, of which, the reverse primer contained a stop codon. Additionally, both of these primers were engineered to include sequences recognized by specific restriction enzymes, EcoRI on the forward primer and NotI on the reverse primer. The use of two different restriction enzymes created different “sticky ends” which upon ligation ensured proper orientation of the insert within the vector. The PCR product was examined with horizontal gel electrophoresis to ensure that the fragment size of about ~2.0 kb (Figure 6A) correlated with the expected size of alpha ENaC (~2.1 kb). The remaining PCR product was cleaned up using the Promega Wizard PCR Clean up kit and then simultaneously digested with EcoRI and NotI. Afterwards the digested PCR product was loaded into a 1% w/v agarose gel, gel extracted by excision, and purified (Figure 6B).

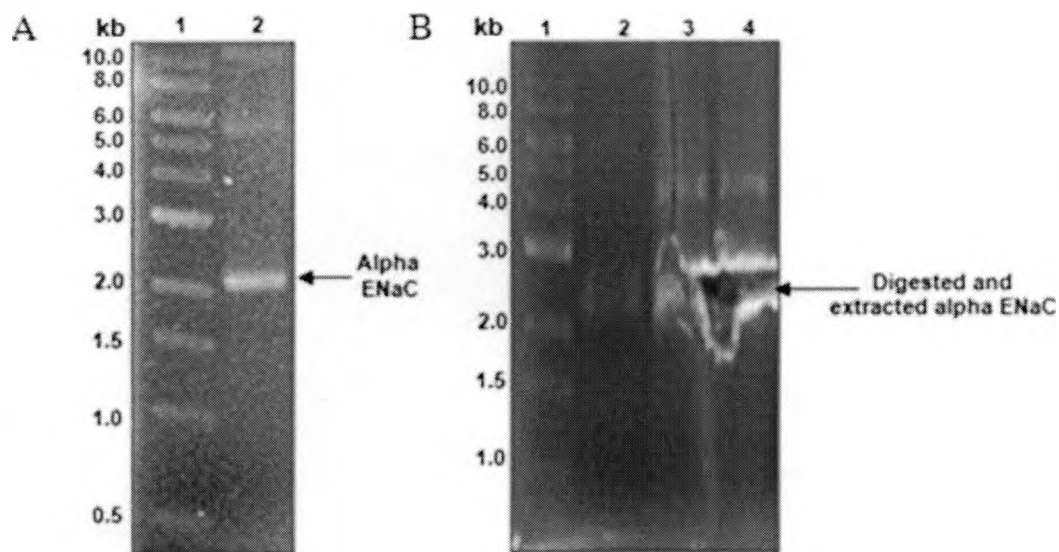


Figure 6: PCR amplification and digestion of the alpha ENaC gene. (A) PCR amplification of alpha ENaC. Lane 1- 1kb ladder and lane 2- alpha-ENaC PCR product. (B) Extraction of digested alpha ENaC. The gel was imaged after extractions. Lane 1- 1kb ladder, lane 2- Uncut alpha-ENaC PCR product, and lanes 3, 4- EcoRI and NotI digested alpha-ENaC PCR product. Both are 1% agarose gels stained with ethidium bromide.

pYES2NT Vector Digestion

The yeast inducible expression vector, pYES2NT, contains an N-terminal purification tag, an Xpress epitope, a galactose promoter, and a uracil auxotrophic gene marker. The pYES2NT vector was selected for two main reasons 1) the expression of alpha ENaC would be controlled and 2) alpha ENaC would contain an N-terminal 6X histidine tag and an Xpress epitope that would allow purification and detection of the fusion protein, respectively (Figure 7). Additionally, since the reverse primer used during PCR included a stop codon, no C-terminal tags would be expressed. Initially, the pYES2NT vector was transformed into *E. coli*, individual colonies were selected and grown for approximately 14 hours, and then the vector DNA was purified using a QIAprep Spin Miniprep kit. Then 6 μ g of pYES2/NT vector was digested with

EcoRI and NotI and treated with calf alkaline phosphatase (CIP) to prevent the digested sticky ends from ligating back together. The digested pYES2/NT vector was visualized as expected at approximately 6.0 kb (Figure 8) on a 1% w/v agarose gel. Digested pYES2/NT DNA was gel extracted and cleaned up.

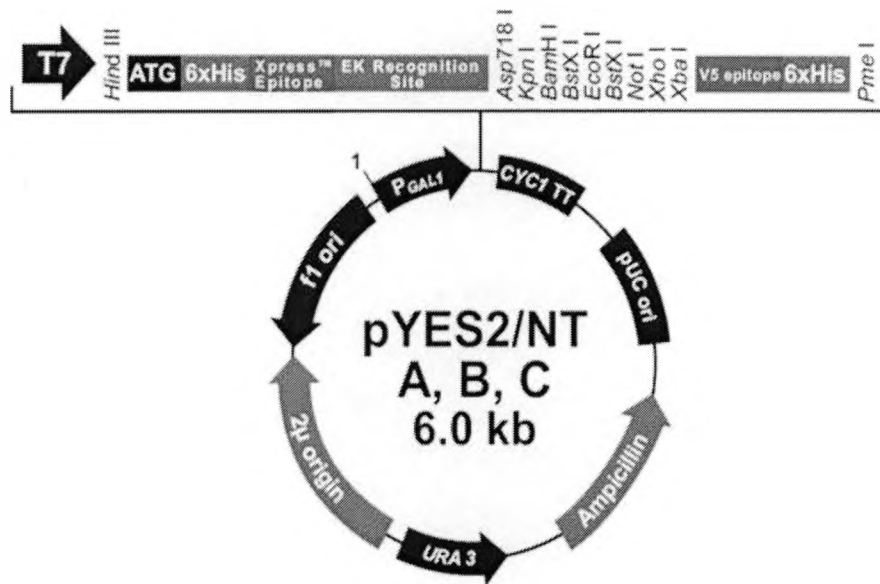


Figure 7: Vector map of pYES2/NT.

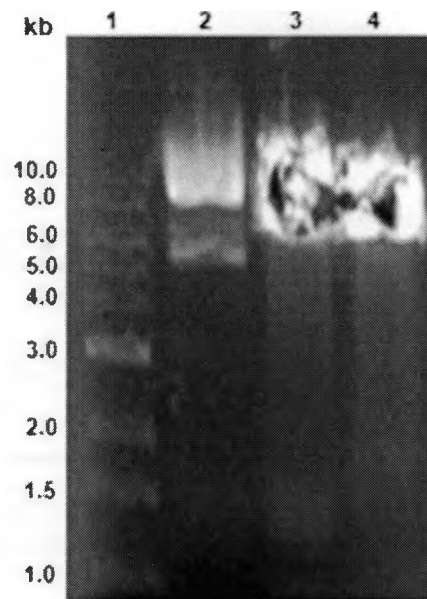


Figure 8: Digestion of pYES2NT DNA. 1% agarose gel stained with ethidium bromide. Lane 1- 1kb ladder, lane 2- uncut pYES2/NT, lanes 3, 4- pYES2/NT digested with EcoRI and NotI. The linear bands in lanes 3 and 4 were excised with tweezers prior to imaging of the gel.

Sub-cloning of Alpha ENaC

A 3:1 ratio of digested and purified PCR amplified alpha ENaC DNA to digested pYES2/NT vector DNA was ligated using T4 DNA ligase. After 30 min this ligation reaction was transformed into competent Top 10 *E. coli* cells, which were then grown on LB agar plates containing ampicillin. Positive transformants were selected, transferred to 5 mL LB broth containing ampicillin, and grown at 37 °C for approximately 16-20 hours. Plasmid DNA was isolated from these overnight cultures using a QIAprep Spin Miniprep kit and analyzed for size in a 1% w/v agarose gel, an initial screen to determine if proper ligation occurred was used in which the migration of the ligated constructs was compared against the migration of empty vector (Figure 9A). Relaxed pYES2/NT containing alpha ENaC was expected to migrate at ~6.0 kb, however pYES2/NT was actually observed at ~4.5 kb because it is supercoiled. pYES2NT-

alpha ENaC was observed at approximately 6.0 kb, which is larger than the vector and certainly within the range of what would be expected for an intact, supercoiled plasmid of ~8.1 kb.

To further examine if cloning was successful a second screen to confirm proper orientation of alpha ENaC was performed. This screen required digesting the pYES2NT-alpha ENaC plasmid with restriction enzymes that would produce fragments of alpha ENaC-pYES2/NT that were distinctive from both vector only and an incorrectly ligated plasmid. An analysis of the pYES2NT-alpha ENaC sequence was performed in order to predict that correct ligation of alpha ENaC into the pYES2/NT vector would produce DNA fragments that migrated at 2.1 kb, 2.7 kb, and 3.3 kb after digestion with AgeI and ClaI. Candidates that passed the first screen were then digested with AgeI and ClaI and analyzed in a 1% w/v agarose gel. Fragments were observed at approximately 2.1 kb, 2.9 kb, and 3.3 kb (Figure 9B), which correspond to the predicted fragment sizes. Additionally, the pYES2NT DNA was also digested with AgeI and ClaI generating a fragment pattern that differed from the digestion of pYES2NT-alpha ENaC.

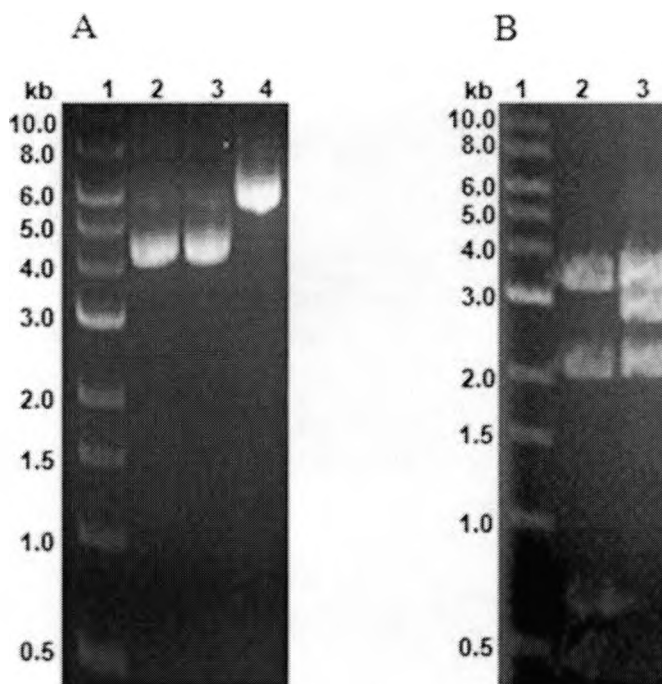


Figure 9: Screen for correctly ligated pYES2NT-alpha ENaC. (A) Initial screen to find plasmids with the alpha ENaC gene inserted. Lane 1-1 kb DNA ladder, lane 2-empty pYES2NT, lane 3-pYES2NT that ligated back together without the gene insert, and lane 4- pYES2NT with the alpha ENaC gene inserted. (B) pYES2NT-alpha ENaC cloning confirmation. Lane 1-1 kb DNA Ladder, lane 2-pYES2NT digested with AgeI and ClaI, and lane 3- pYES2NT-alpha ENaC digested with AgeI and ClaI. Both are 1% w/v gels stained with ethidium bromide.

pYES2/NT-alpha ENaC clones that passed both screens were then re-transformed, isolated, and submitted for DNA sequencing in concentrations that were approximately 600 to 800 ng/ μ L. Three sequencing primers were used to ensure complete coverage of the alpha ENaC gene: a *GALI* forward primer, an internal primer specific to alpha ENaC, and a V5 reverse primer. The sequence obtained from each primer was then compared to the known sequence of alpha ENaC to check for mutations and/or insertions. A confirmed pYES2/NT-alpha ENaC clone (Figure 10) was used for all subsequent studies including expression of alpha ENaC.

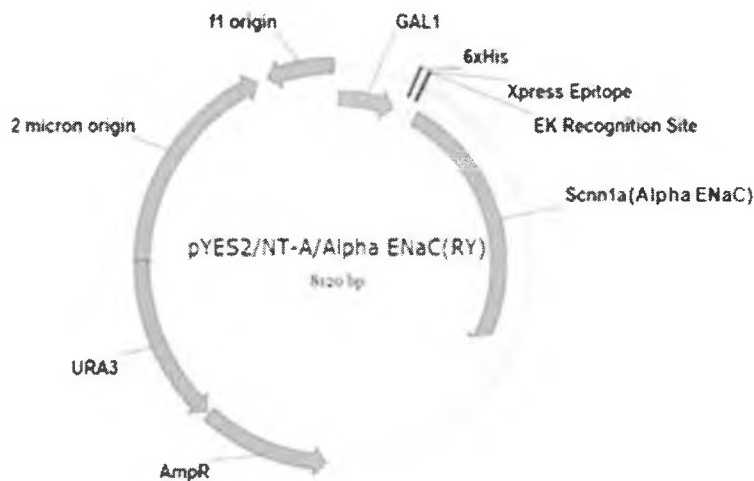


Figure 10: Vector map of pYES2NT-alpha ENaC

Alpha ENaC Expression

The pYES2/NT-alpha ENaC plasmid was transformed into both competent *S. cerevisiae* strains S1InsE4A and BY4742 for expression of alpha ENaC. Individual yeast colonies from the transformations were selected and grown for approximately 16-20 hours at 30 °C in synthetic media containing 2 % w/v glucose as a sugar source. The culture media was then changed to synthetic media containing 2% w/v raffinose as a sugar source and grown an additional 16-20 hours. OD₆₀₀ readings were taken to determine the cell density and these readings were then used to inoculate synthetic media containing 2 % w/v galactose at an OD₆₀₀ of 0.4. These cultures were then grown for 6-8 hours with shaking at 30 °C. Afterwards, cells were pelleted and frozen at -20 °C.

To lyse the yeast cells and extract proteins, the cells were resuspended in standard breaking buffer to obtain an OD₆₀₀= 200 and vortexed in the presence of acid-washed glass beads

cells. After removal of the cellular debris by centrifugation, an aliquot of cellular proteins was loaded into a 7.5% Tris-glycine SDS-PAGE and transferred onto a nitrocellulose membrane. In order to view alpha ENaC expression, the membrane was probed with anti-Xpress primary antibody. Detection required the use of an HRP conjugated secondary antibody which luminesces in the presence of its substrates; this luminescence was detected by exposing it to X-ray film. Alpha ENaC was observed in both yeast strains with similar expression at 6 hours with both exhibiting three bands at 95 kDa, 105 kDa, and 113 kDa (Figure 11). In mammalian cells ENaC is usually expressed as a 90 kDa polypeptide; the triplicate band observed in yeast may be due to varied glycosylation of alpha ENaC in yeast. It is known that the synthesis and processing of N-linked glycans by yeast differs from that of higher organisms, with the major difference occurring in the 'late processing' stages that take place in the Golgi apparatus (31). Yeast typically utilize the high mannose type of N-linked glycosylation whereas mammalian cells usually contain the complex types. Therefore it is to be expected that eukaryotic proteins expressed in yeast will most likely have differing glycosylation patterns. As for ENaC, it is well documented that in mammalian cells ENaC is assembled and core glycosylated in the ER, but what remains unclear is if and how ENaC is processed in the Golgi apparatus (17,32).

Only one other report, Canessa *et al.*, has described expression of ENaC in yeast. They reported a molecular weight of 140 kDa for an $\alpha\beta$ ENaC fusion protein in *S. cerevisiae* TF23 (26). Like alpha ENaC, beta ENaC has a reported molecular weight at ~90 kDa. The difference between our reported weight and theirs may be due to differences in glycosylation and that expression of a fusion protein results in different glycosylation of ENaC by yeast.

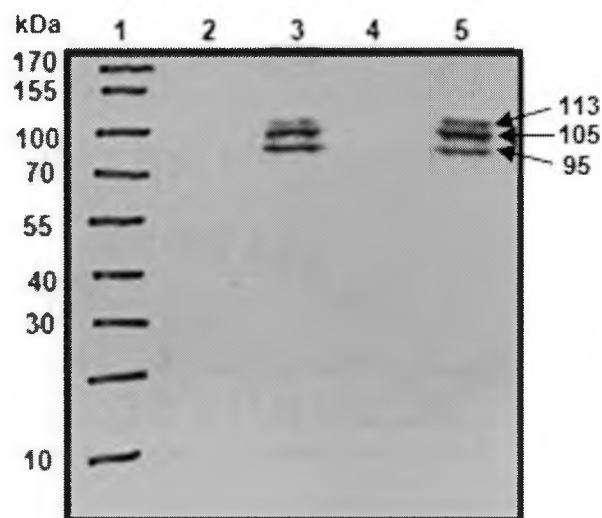


Figure 11: Western blot of alpha ENaC expression in *S. cerevisiae*. Lane 1- protein standard marker, lane 2- pYES2/NT (Control) expressed in S1InsE4A, lane 3- pYES2NT-alpha ENaC expressed in S1InsE4A, lane 4- pYES2/NT (Control) expressed in BY4742, and lane 5- pYES2NT-alpha ENaC expressed in BY4742. Blot was probed with anti-Xpress primary antibody and anti-mouse-HRP secondary antibody and detected with by using a Western Lightning Kit to detect HRP activity.

Expression of Alpha ENaC Confers Salt Sensitivity to Yeast

After confirmation of alpha ENaC expression, we next aimed to demonstrate that expression of alpha ENaC would confer salt sensitivity to yeast indicating proper assembly and function of the channel at the membrane. To examine salt sensitivity in yeast a dilution pronging survival assay was performed. *S. cerevisiae* were grown for 2-3 days on selective synthetic media containing raffinose in order to produce a sufficient number of cells for the assay. Cells were harvested from synthetic media plates containing 2% raffinose, quantitated with a hemocytometer, and then an aliquot containing 1×10^7 cells were diluted 5-fold across the length of a 96 well plate. The cells were then pronged onto selective synthetic media containing

galactose to induce expression of alpha ENaC. Pronged plates were then incubated at 30 °C for 3-6 days before imaging.

When ENaC was pronged onto selective synthetic media containing glucose, growth was similar to pYES2NT (Control) because expression of ENaC is repressed (Figure 12A). However when ENaC was pronged onto galactose, expression of ENaC is induced resulting in slight growth inhibition (Figure 12B). This effect was amplified and made even more apparent when grown in the presence of high salt (1 M NaCl) (Figure 12C). Other concentrations of salt (0.1 M, 0.3 M, 0.5 M, and 1.5 M NaCl) were also examined (data not shown) and effective growth inhibition occurred in the 0.5 M-1.0 M range, with concentrations above 1.0 M being lethal to the cells.

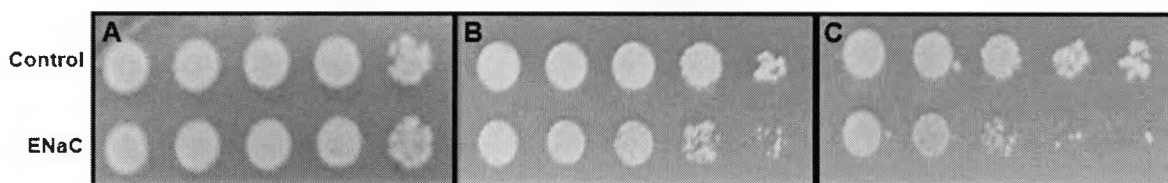


Figure 12: Dilution pronging to assay salt sensitivity. *S. cerevisiae* S1InsE4A transformed with pYES2NT (Control) or pYES2NT-alpha ENaC (ENaC) on glucose (A), galactose (B), and (C) galactose + 1 M NaCl media.

Growth in liquid media was also examined for differences in growth between yeast cells transformed with pYES2NT (Control) or pYES2NT-alpha ENaC. This required growing yeast cells for approximately 16-20 hrs in synthetic media containing 2% w/v glucose as a sugar source with the additional salt (0.5 M NaCl) when appropriate. The next day the culture media was changed to synthetic media containing 2% w/v raffinose as a sugar source and the additional salt when appropriate and grown another 16-20 hrs. OD₆₀₀ readings were taken to determine the

cell density and these readings were then used to inoculate synthetic media containing 2% w/v galactose and the additional salt when appropriate at an OD_{600} of 0.4. Growth curves were constructed by measuring the absorbance at 600 nm every 2 hrs for 8 hours followed by a reading at 24 hrs (Figure 13). *S. cerevisiae* transformed with either pYES2NT or pYES2NT-alpha ENaC grew well under low salt conditions, with *S. cerevisiae* transformed with pYES2NT-alpha ENaC showing a slight reduction in growth at ~12%. However, in the presence of 0.5 M NaCl, *S. cerevisiae* transformed with pYES2NT-alpha ENaC exhibited a 42% reduction in growth after 24 hrs when compared to control cells in the presence of salt. Growth curves were also examined in 1 M NaCl, but neither type of cell was able to grow under this high salt condition in liquid media.

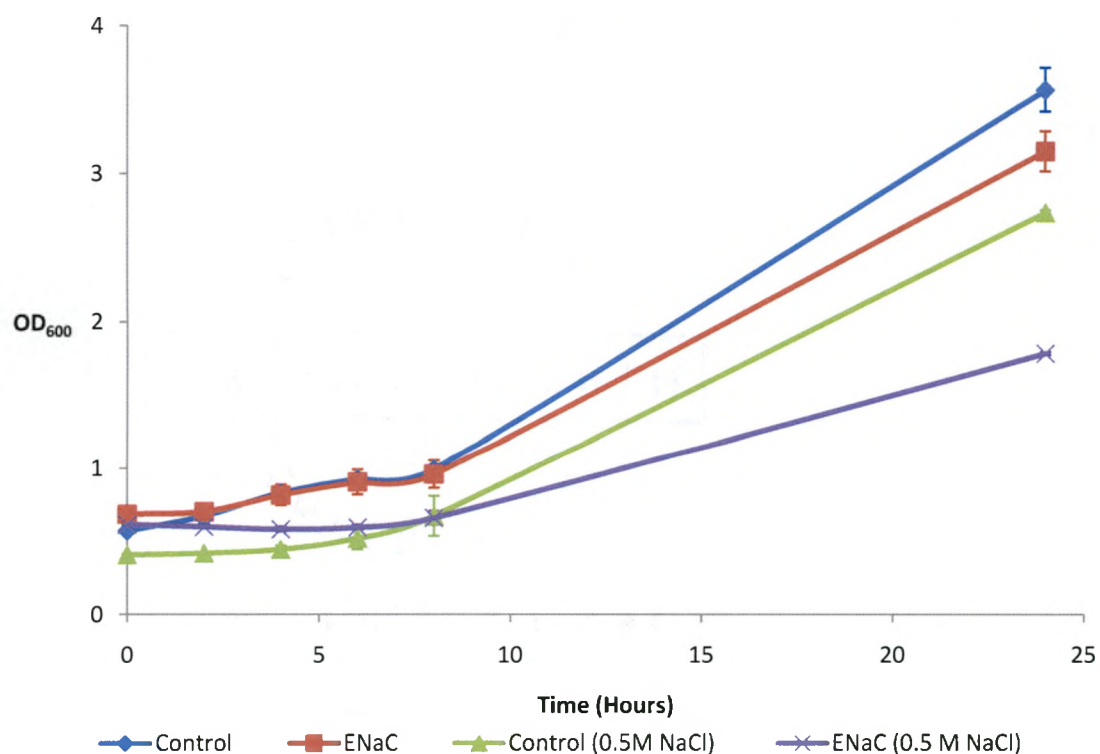


Figure 13: Growth curves to assay salt sensitivity. *S. cerevisiae* cells transformed with pYES2NT (Control) or pYES2NT-alpha ENaC (ENaC) with and without the addition of 0.5 M NaCl. The cells were grown at 30 °C for 24 hrs and the OD_{600} was recorded at regular intervals. Error bars indicate standard error (n=3).

Membrane localization is required for ENaC to be functional, i.e. to pump sodium into the cell. Therefore, to generate further evidence that ENaC expression in yeast generated functional channels at the membrane, yeast cells transformed with either pYES2NT or pYES2NT-alpha ENaC were analyzed with immunocytochemistry (unpublished results of Lyndsey Kirk). Previous work with expressing ENaC in a yeast expression system utilized a pYES2.1TOPO expression system, but neither membrane localization (Figure 14A) nor salt sensitivity was observed with these cells (unpublished results of Mikki Boswell). However when pYES2NT-alpha ENaC transformed cells were examined with the confocal microscope the fluorescence is localized to the membrane (Figure 14B) indicating that ENaC processing in yeast results in a channel that correctly localizes to the membrane. We hypothesize that placing a purification tag on the C-terminal end of alpha ENaC may interfere with signaling sequences that aid yeast cells in delivering ENaC to the cell membrane.

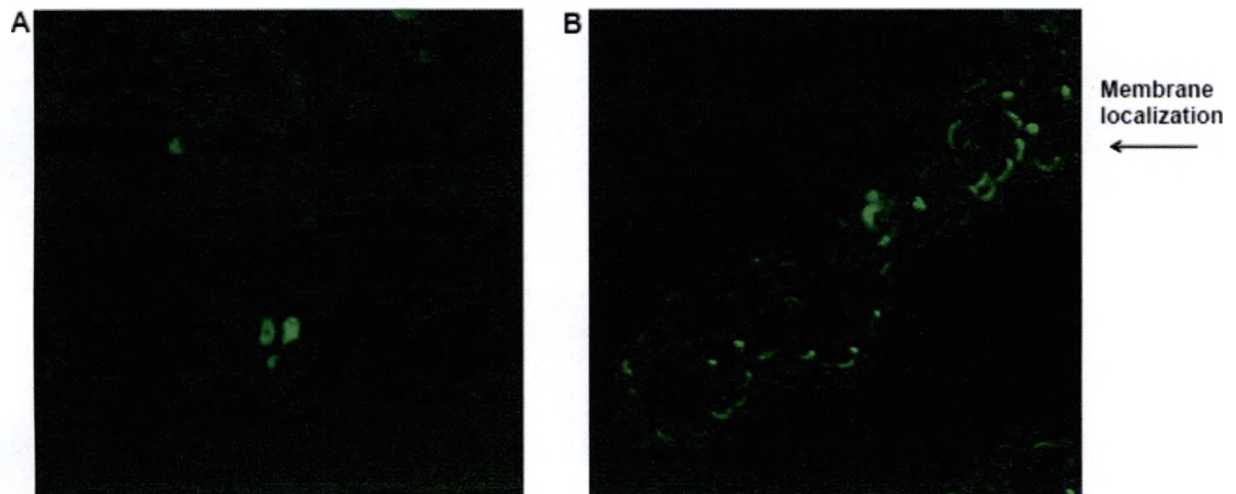


Figure 14: Immunocytochemistry of *S. cerevisiae* expressing alpha ENaC. (A) For comparison, when C-terminal alpha ENaC fusion protein (non-functional) is expressed and probed with anti-V5 antibody membrane localization is not observed (B) Cells containing pYES2NT-alpha ENaC fluoresce at the membrane. Images were taken at 40x with immersion oil using an Olympus 1X70 microscope with BioradMR1024 laser scanning confocal microscope. An anti-mouse alexaflour-488 was used as a secondary antibody.

Amiloride Rescue

Amiloride is a blocker of ENaC channels at submicromolar levels (10). We hypothesized that if salt sensitivity is a phenotype conferred by functioning alpha ENaC channels, then the presence of amiloride in the media should block ENaC activity and result in improved growth rates. This hypothesis was tested by comparing growth between yeast transformed with the pYES2/NT-alpha ENaC plasmid and yeast transformed with pYES2/NT with increasing concentrations of amiloride in both solid and liquid synthetic media containing galactose. To examine amiloride rescue in solid media a dilution pronging assay was carried out. In the preparation of the pronging amiloride in varied concentrations was added to the well plate prior to pronging to the agar plate, however even at low concentrations of salt (0.1 M) we were not able to demonstrate growth that matched the control (Figure 15).

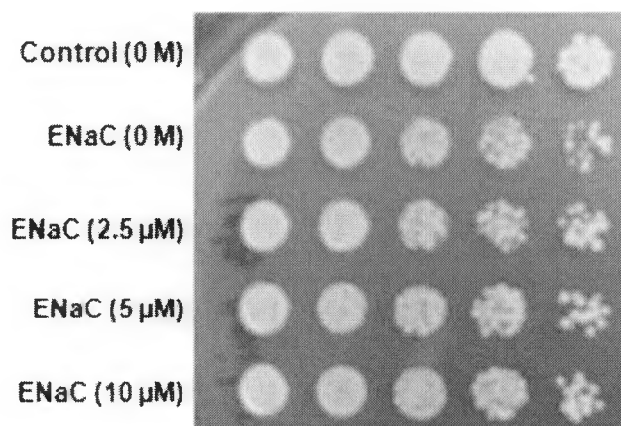


Figure 15: Dilution pronging to assay amiloride rescue. *S. cerevisiae* S1InsE4A transformed with pYES2NT (Control) or pYES2NT-alpha ENaC (ENaC) in the presence of varying concentrations of amiloride on galactose + 0.1 M NaCl. The plate was imaged 3 days after the initial pronging.

Growth was also examined in liquid media. This required inoculating synthetic media containing 2% w/v glucose as a sugar source with yeast transformed with pYES2/NT and

pYES2/NT-alpha ENaC and incubating for 16-20 hours at 30 °C with shaking. The culture media was then changed to synthetic media containing 2% w/v raffinose as a sugar source and grown an additional 16-20 hours. OD₆₀₀ readings were taken to determine the cell density and these readings were then used to inoculate synthetic media containing 2 % w/v galactose at an OD₆₀₀ of 0.4. The following conditions: 0 M NaCl, 0.5 M NaCl plus 2.5 μM amiloride, 0.5 M NaCl plus 5.0 μM amiloride, and 0.5 M NaCl plus 10.0 μM amiloride were examined. The controls neither contained NaCl nor amiloride and each condition was carried out in duplicate. The strains were grown at 30 °C for 24 hours and final OD₆₀₀ values were recorded.

As with the solid media, we were not able to clearly demonstrate recovery of salt tolerance in cells expressing ENaC, but we do observe partial recovery. We believe that the differences between the two tests is due to the length of time required to take the measurements, one day for liquid media as opposed to 3-6 days with solid media. In the liquid media amiloride test, the control cells appeared to be affected by both high salt and amiloride, with salt causing growth inhibition in general. On the other hand, amiloride appeared to aid the control cells in tolerating these higher salt conditions (Figure 16). Yeast expressing ENaC did appear to grow better in high salt in the presence of 2.5 and 5 μM amiloride and their growth was similar to control cells grown in high salt without amiloride. At 10 μM cells growth decreases and this could be due to a negative effect on native yeast channels. The positive affect that amiloride appears to have on the salt tolerance of yeast in general makes it difficult to say that we have demonstrated recovery of function for ENaC expressing cells. However, the results do demonstrate at least partial recovery of function independent of the positive effect amiloride seems to have on yeast tolerance of high salt conditions.

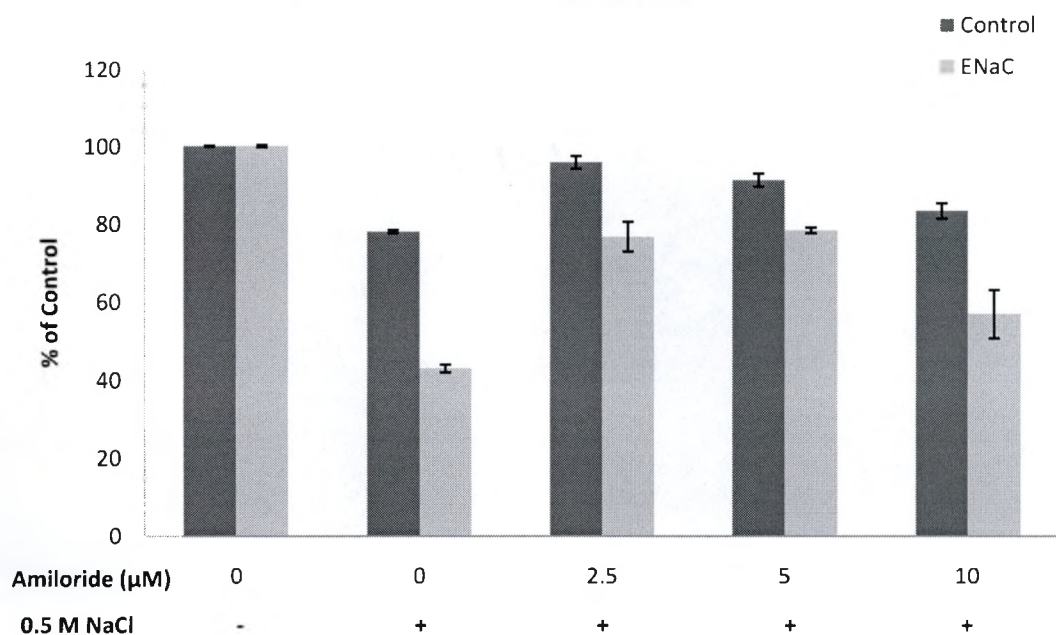


Figure 16: The effects of amiloride on growth. Growth curves of *S. cerevisiae* transformed with pYES2NT (Control) or pYES2NT-Alpha ENaC (ENaC) in galactose + 1 M NaCl. ENaC expression is only induced when grown on galactose containing media. The cells were grown at 30 °C for 24 hr. Error bars indicate standard error (n=2).

Expression of Alpha ENaC Mutants Results in Variable Growth

The salt sensitivity phenotype resulting from alpha ENaC expression was used to examine residues critical for ENaC function. Five alpha ENaC mutants of known function in mammalian cells were screened for salt sensitivity using the pYES2/NT expression system. They were F111I and A113I, both similar in function to wild type ENaC, W112C, which is 10-20% less active than wild type, and W112K and His1, which were both inactive mutants. Experimental data was provided by J. Stockand (personal communication, April 7, 2009) who made mutant function determinations based on patch clamp analysis of mutants expressed in Chinese hamster ovary (CHO) or simian kidney (COS) cells. All mutations are point mutations except, His1, which is a mutant with an inserted 6XHis tag sequence in the cytosolic region.

Utilizing these mutants in our screen first required sub-cloning each mutant alpha ENaC gene. This was performed in a similar manner as described before for wild-type alpha ENaC. In brief, mutant alpha ENaC genes were amplified with PCR utilizing the wild-type primers, digested with EcoRI and NotI, and ligated into pYES2/NT vector that was also digested with EcoRI and NotI. Two screens were employed to determine correct ligation of the genes into the vector 1) screen for correct molecular weight and 2) digestion with AgeI and ClaI to produce fragments determined by sequence analysis. The cloning confirmation of pYES2NT- His1-alpha ENaC is shown (Figure 17) as an example, but all ENaC mutants produced similar gel patterns.

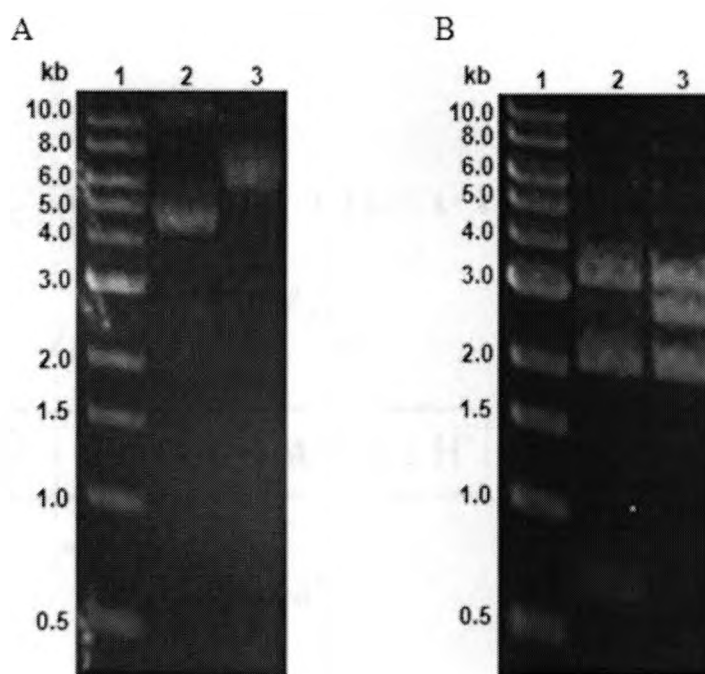


Figure 17: Screen for correctly ligated pYES2NT-His1-alpha ENaC. (A) Initial screen to find plasmids with the His1-alpha ENaC gene inserted. Lane 1-1 kb DNA ladder, lane 2-empty pYES2NT, lane 3- pYES2NT-His1-alpha ENaC. (B) Cloning confirmation with digestion. Lane 1-1 kb DNA Ladder, lane 2-pYES2NT digested with AgeI and ClaI, and lane 3-pYES2NT-His1-alpha ENaC digested with AgeI and ClaI. Both are 1% w/v gels stained with ethidium bromide.

Each mutant pYES2NT- α ENaC plasmid was transformed into both *S. cerevisiae* S1InsE4A and BY4742 cells and assayed using a dilution pronging. We predicted that various levels of ENaC function due to mutations would result in yeast cells with variable salt sensitivities. These results would then be easily compared through the use of a dilution pronging survival assay. Initially the dilution pronging was carried out using S1InsE4A *S. cerevisiae*, but differences between the mutant strains were not easily distinguishable. However when BY4742 cells were used in the pronging dilution assay our results demonstrated various levels of salt sensitivity (Figure 18). There were three cases that did not match the expected level of activity. The mutations A113I and F111I were expected to display results similar to wild type; however the pronging assays show that these grow better than wild type. This indicates that in yeast these mutations result in a less active form of ENaC. His1 was expected to be inactive and the results indicate that in yeast this mutant is active.

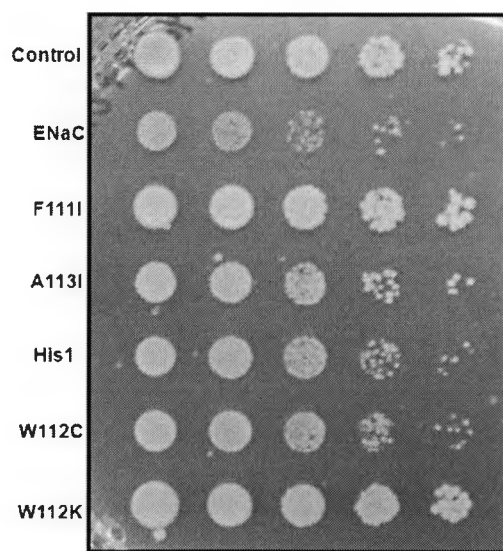


Figure 18: Dilution pronging assay of α ENaC mutants. *S. cerevisiae* BY4742 transformed with pYES2NT (control), pYES2NT- α ENaC (ENaC), pYES2NT- F111I- α ENaC (F111I), pYES2NT- A113I- α ENaC (A113I), pYES2NT- His1- α ENaC (His1), pYES2NT- W112C- α ENaC (W112C), and pYES2NT- W112K- α ENaC (W112K) were assayed on galactose + 1 M NaCl media.

Expression of the alpha ENaC mutants was also examined with a western blot analysis that was carried out in a similar manner as described before (Figure 19). When the data are compared to that of the dilution pronging several interesting observations can be made. Mutant F111I has a function similar to wild type in mammalian cells, but in yeast it appears to be less active than wild type resulting in less salt sensitivity when grown in yeast. When these cells were analyzed with western blotting this result we observed less expression than wild type ENaC, suggesting that reduced protein levels rather than reduced activity caused the phenotype. Mutant A113I also has a function similar to wild type in mammalian cells, but in yeast it appears to be less active than wild type also resulting in less salt sensitivity when grown in yeast. However, when A113I cells were analyzed with western blotting the result was increased expression when compared to wild type ENaC. One fault in using western blotting to analyze expression is that the technique does not distinguish between ENaC expressed in the cytosol versus at the membrane. For the A113I mutation, one explanation for this contradictory result could be that in yeast expression of A113I ENaC results in more expression than wild type, but that either fewer channels localize to the membrane and/or they are less active in the yeast system.

On the other hand W112C, W112K, and His1 are mutations to ENaC that result in a less active or inactive channel in mammalian cells. In yeast, expression of W112C ENaC also resulted in a less functional channel which was demonstrated by improved growth as compared to wild type ENaC in the dilution pronging. Western blotting showed that W112C demonstrated a similar expression profile indicating that the channel may be expressed in a similar manner, but that the mutation may affect the rate of sodium uptake. In contrast, W112K, an inactivating substitution resulted in diminished expression when compared to wild type. This low level of expression coincides with the dilution pronging data where this mutation demonstrated a growth

pattern very similar to the control strain that lacks ENaC entirely. Lastly, the His1 mutation, which resulted in an inactive form of ENaC in mammalian cells, appeared to have an opposite effect in yeast. This substitution is unlike the others in that rather than being a single point mutation, this mutation is the result of an added 6X His tag on the extracellular loop of ENaC. In yeast this mutation is less active than wild type resulting in less salt sensitivity, but not quite the rate of growth demonstrated by the control strain that lacks ENaC entirely. The expression pattern differs from wild type as well suggesting that locating a His tag on the extracellular loop of ENaC interferes with sodium transport in the yeast expression system as well, but not to the point where the channel is completely inactivated.

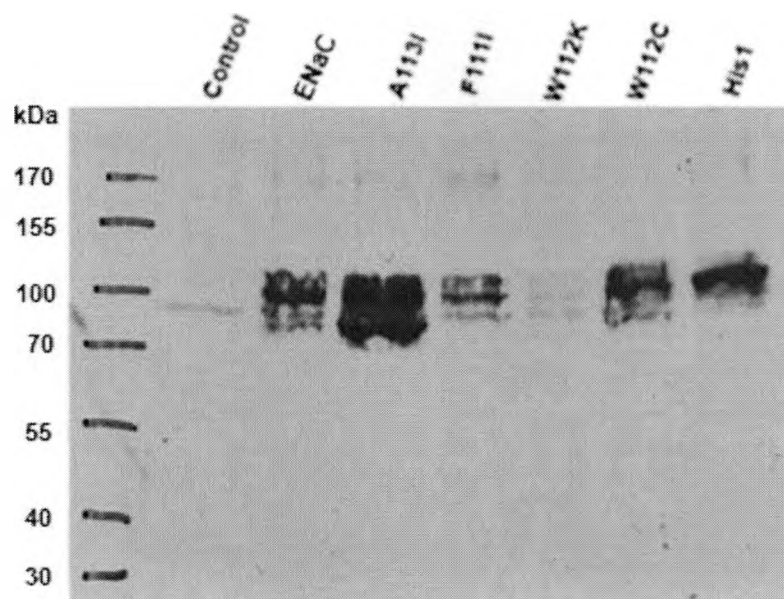


Figure 19: Western blot of alpha ENaC mutants. Lane 1 is a Fermentas protein standard marker, lane 2 is pYES2/NT (Control), lane 3 is pYES2NT-alpha ENaC (ENaC), lane 4 is pYES2NT- A113I-alpha ENaC(A113I), lane 5 is pYES2NT- F111I-alpha ENaC (F111I), lane 6 pYES2NT- W112K-alpha ENaC (W112K), lane 7 is pYES2NT- W112C-alpha ENaC (W112C), and lane 8 pYES2NT- His1-alpha ENaC (His1).

While our results do not correlate exactly with function in mammalian cells (Table 5), we are able to detect differences in both the dilution pronging and western blots of the different mutants. Further examination of the mutant forms will be required to assess how expression differs at the membrane. We plan to pursue the examination of mutant function at the membrane through the use of a membrane biotinylation assay (33). Despite the results we maintain that the screen will still be useful in identifying interesting mutations in ENaC, but that these mutations will require follow up studies conducted in the traditional mammalian expression systems.

Table 5: Summary of mutant alpha ENaC functions.

Mutant	Function (Mammalian Cells)	Dilution Pronging Results (Yeast)	Expression Levels (Yeast)
F111I	Similar to wild type	Reduced activity/Inactive	Slightly lower than wild type
A113I	Similar to wild type	Slightly less active	Higher than wild type
His1	Inactive	Slightly less active	Similar to wild type
W112C	10-20% less active	Slightly less active	Similar to wild type
W112K	Inactive	Inactive	Lower than wild type

Screening the Yeast Deletion Library

Another advantage of using a yeast expression system is the fact that the yeast genome has been well characterized. As a result, the *Saccharomyces* Genome Deletion Project has generated a collection or library of strains in which one gene has been deleted which are commercially available in a *S. cerevisiae* BY4742 background. Therefore we aimed to determine if this deletion library could be used to identify proteins necessary for ENaC channel function. The deletion library contains over 5000 strains, however only 7 strains were examined in this

initial screen (Table 6). The strains examined were selected because they have been shown to affect expression of inwardly rectifying potassium (Kir) channels and while Kir channels differ from ENaC channels, both are ion channels that require processing and packaging in the ER (27).

Table 6: Summary of deletion strains used in the ENaC screen.

Name	ORF	Function	Dilution Pronging Results (Yeast)
<i>SUR4</i>	YLR372W	Elongase; involved in fatty acid biosynthesis (34)	Less active than wild type
<i>CSG2</i>	YBR036C	Endoplasmic reticulum (ER) membrane protein, required for mannosylation of inositolphosphorylceramide (35)	Similar to wild type
<i>ERV14</i>	YGL054C	Involved in vesicle formation and incorporation of specific secretory cargo (36)	Less active than wild type
<i>EMP24</i>	YGL200C	Integral membrane component of ER-derived COPII-coated vesicles, involved in ER to Golgi transport (37)	Less active than wild type
<i>ERV25</i>	YML012W	Protein that complexes with Erp1, Erp2p, and Emp24; involved in ER to Golgi transport (37)	Less active than wild type
<i>UBA3</i>	YPR066W	Protein that acts together with Ula1p to activate Rub1p before its conjugation to proteins (neddylation), which may play a role in protein degradation (38)	Similar to wild type
<i>ULA1</i>	YPL003W	Protein that acts together with Uba3p to activate Rub1p before its conjugation to proteins (neddylation), which may play a role in protein degradation (38)	More active than wild type

The strains selected were transformed with pYES2NT-alpha ENaC and assayed using dilution pronging. The dilution pronging showed that of the seven strains examined, only four appeared to cause a reduction in growth inhibition indicating that these gene deletions may impair ENaC function and/or processing (Figure 20). These were *SUR4* (YLR372W), *ERV14*

(YGL054C), *EMP24* (YGL200C), and *ERV25* (YML012W). Additionally, of the seven examined, only one, *ULAI* (YPL003W), showed significant reduction in growth suggesting an overly active ENaC or an increased stability of otherwise normal channels.

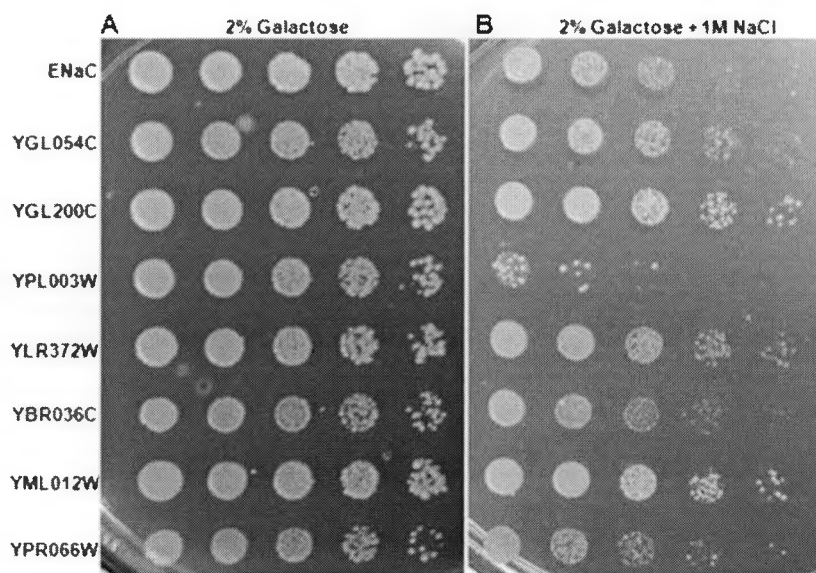


Figure 20: Dilution pronging assay of deletion strains. *S. cerevisiae* BY4742 deletion strains transformed with pYES2NT-alpha ENaC (ENaC) and grown on galactose (A) and (B) galactose with 1 M NaCl added.

SUR4 is a protein involved in the synthesis of 26-carbon long chain fatty acids, and while it can elongate several substrates, it is essential for the conversion of 24-carbon to 26-carbon fatty acids. Deletion of *SUR4* changes the composition of these long chain fatty acids, which serve as precursors for ceramide and sphingolipids, and can alter the composition of the membrane lipid bilayer. One way in which the deletion of *SUR4* could impair ENaC function could be disruption of lipid rafts. Lipid rafts are domains within membranes made of cholesterol and sphingolipids. They are often associated with the targeting of proteins sequestered in them. It

is unclear exactly how ENaC is delivered to the cell membrane, but there is evidence that lipid rafts may be involved. Hill *et al.* have reported the involvement of lipid rafts in both A6 cells, a *Xenopus* kidney cell line, and in mouse cortical collecting duct cells they were able to detect 30% of ENaC in lipid rafts (39,40). Lipid rafts are found in yeast (41), and thus this may explain better growth in a *SUR4* deletion strain if ENaC is utilizing lipid rafts for delivery to the membrane.

The other deletion strains that showed improved growth were *ERV14* (YGL054C), *EMP24* (YGL200C), and *ERV25* (YML012W). Proteins encoded by these genes are all involved in the packaging of proteins into transport vesicles in order to exit the ER (36,37). ENaC is assembled and glycosylated in the ER initially before being transported out. Thus these gene deletions that alter the exit of protein out of the membrane could in fact decrease ENaC function by inhibiting ENaC exit from the ER.

Notably, when *ULA1* (YPL003W) cells were transformed with alpha ENaC a reduction in growth was observed. The ULA1 protein plays a role in the yeast degradation system; it is required for assembly of RUB1, a ubiquitin-like protein. As for ENaC, normal degradation of ENaC occurs when an ubiquitin tag is added. *ULA1* may code for a protein that allows yeast cells to signal for alpha ENaC degradation; without this signal ENaC is not degraded causing increased salt sensitivity in yeast.

CHAPTER IV

CONCLUSIONS

Yeast cells have been extensively reported as a eukaryotic model system for a variety of mammalian proteins, including ion channels. Yeast, like bacteria are well characterized, easily manipulated, and can carry a variety of selectable markers; unlike bacteria, they possess a glycosylation system, a post-translational modification that many eukaryotic proteins require in order to be functional. Additionally, many yeast strains are able to tolerate high levels of salt (1 M) as they have coping abilities for extruding sodium ions, which is toxic to yeast because it replaces potassium ions in enzymatic processes. Based on all of this information, we hypothesized that yeast may serve as a viable expression system for alpha ENaC, a mammalian ion channel that requires glycosylation.

We used a variety of techniques, such as dilution pronging, immunocytochemistry, and immunoblotting to demonstrate that yeast are able to express wild type alpha ENaC properly localized to the membrane and that salt sensitivity was conferred to yeast cells indicating a functional channel. We next developed a quick screen of alpha ENaC function in yeast which requires cloning alpha ENaC or a mutant of alpha ENaC into the pYES2NT expression system, transforming the newly constructed plasmid into *S. cerevisiae* BY4742 cells, and then performing a dilution pronging assay on yeast agar plates containing galactose and 1 M NaCl. We used five different alpha ENaC mutants to evaluate the effectiveness of our screen. When

ENaC mutants were assayed with our screen differences in salt sensitivity were detected, but we observed that our screen does not exactly mimic the function of ENaC mutants in mammalian cells. Despite this, we maintain that it can still be used to identify potential residues critical to proper ENaC function, but that follow up studies in mammalian cells will be required.

Additionally, there is another advantage of using a yeast expression system over a traditional mammalian expression system which lies in the ability to easily select for yeast cells through the use of a selectable marker. When mammalian cells are transfected cells may uptake variable amounts of DNA and some cells will not contain any at all. This makes comparing expression levels in mammalian cells quite challenging. However with this screen in yeast all cells contain comparable amounts of the plasmid when grown on selective media. Studying ENaC in yeast may provide an easier mechanism for examining differences in expression and evaluating how mutations may affect the pool of ENaC that reaches the membrane.

We additionally reported that the screen can be used to search for genes that may be required for the proper processing and expression of alpha ENaC at the membrane. Yeast cells share many conserved metabolic pathways with mammalian systems and genes that are required for expression of functional ENaC may have mammalian counterparts. The viability of screening deletion mutants from the *Saccharomyces* Genome Deletion Project was examined by using this expression system to examine seven deletion mutants. Of the seven strains examined, four strains exhibited increased growth when compared to wild type: *SUR4*, *ERV14*, *EMP24*, and *ERV25*. This loss in salt sensitivity is likely to be due to loss in ENaC function or localization indicating that these genes are required for proper ENaC function.

This study has shown that it is possible to express functional alpha ENaC in yeast cells and assay the salt sensitivity in a dilution pronging to screen mutants or deletion strains. In the

future this screen can be used to further examine alpha ENaC mutants leading to insights into its function or structure. The screen may also be used to search for genes that may affect alpha ENaC function and/or expression, further providing insight into ENaC's physiological role.

REFERENCES

- (1) Niemeier, B. A., *et al. EMBO reports* **2001**, *2*, 568-573.
- (2) Burnier, M. *Sodium in Health and Disease*; CRC Press, 2007.
- (3) Meneton, P.; Loffing, J.; Warnock, D. G. *Am J Physiol Renal Physiol* **2004**, *287*, F593-601.
- (4) Kellenberger, S.; Schild, L. *Physiol Rev* **2002**, *82*, 735-767.
- (5) Kokko, J. P. In *Encyclopedia of Life Sciences*; John Wiley & Sons, Ltd: 2001.
- (6) McDonald, F. J.; Price, M. P.; Snyder, P. M.; Welsh, M. J. *Am. J. Physiol.* **1995**, *268*.
- (7) Stockand, J. D., *et al. IUBMB Life* **60**, 620-628.
- (8) Itzhak Mano, M. D. *BioEssays* **1999**, *21*, 568-578.
- (9) Kellenberger, S.; Schild, L. **2002**, 735-767.
- (10) Kellenberger, S.; Gautschi, I.; Schild, L. *Mol Pharmacol* **2003**, *64*, 848-856.
- (11) Schild, L.; Schneeberger, E.; Gautschi, I.; Firsov, D. *J. Gen. Physiol.* **1997**, *109*, 15-26.
- (12) Jasti, J.; Furukawa, H.; Gonzales, E.; Gouaux, E. *Nature* **2007**, *449*, 316-323.
- (13) Starchenko, A.; Adams, E.; Booth, R. E.; Stockand, J. *Biophysical Journal* **2005**, *88*, 3966-3975.
- (14) Randrianarison, N., *et al. J Physiol* **2007**, *582*, 777-788.
- (15) Harris, M., *et al. J. Biol. Chem.* **2008**, *283*, 7455-7463.
- (16) Hager, H., *et al. Am J Physiol Renal Physiol* **2001**, *280*, F1093-1106.

- (17) Butterworth, M. B.; Weisz, O. A.; Johnson, J. P. *J. Biol. Chem.* **2008**, *283*, 35305-35309.
- (18) Snyder, P. M. *Endocrine Reviews* **2002**, *23*, 258-275.
- (19) Vallet, V., *et al.* *Nature* **1997**, *389*, 607-610.
- (20) Kleyman, T. R.; Carattino, M. D.; Hughey, R. P. *J. Biol. Chem.* **2009**, R8000-83200.
- (21) Bengrine, A.; Li, J.; Hamm, L. L.; Awayda, M. S. *J. Biol. Chem.* **2007**, *282*, 26884-26896.
- (22) Lifton, R. P.; Gharavi, A. G.; Geller, D. S. *Cell* **2001**, *104*, 545-556.
- (23) Lifton, R. P. *PNAS* **1995**, *92*, 8545-8551.
- (24) Nakamura, R. L.; Gaber, R. F. *Methods Enzymol* **1998**, *293*, 89-104.
- (25) Giaever, G., *et al.* *Nature* **2002**, *418*, 387-391.
- (26) Gupta, S. S.; Canessa, C. M. *FEBS Letters* **2000**, *481*, 77-80.
- (27) Haass, F. A.; Jan, L. Y.; Shulder, M. *PNAS* **2007**, *104*.
- (28) Brachmann, C. B.; Cost, G.C.; Caputo, E.; Li, J.; Hieter, P.; Boeke, J. D. *Yeast* **1998**, *14*, 115-132.
- (29) Morrison, A.; Johnson, A. L.; Johnson, L. H.; and Sugino, A. *EMBO J.* **1993**, *12*, 1467-1473.
- (30) Ybanez, R. V.; Boswell, M. G.; Booth, R. E. *FASEB J.* **2009**, *23*, 698.6.
- (31) Kukuruzinska, M. A.; Bergh, M. L. E.; Jackson, B. J. *Annual Review of Biochemistry* **1987**, *56*, 915-944.
- (32) Rotin, D.; Kanelis, V.; Schild, L. *Am J Physiol Renal Physiol* **2001**, *281*, F391-399.
- (33) Klis, F. M.; de Jong, M.; Brul, B.; de Groot, P. W. J. *Yeast* **2007**, *24*, 253-258.
- (34) Oh, C. S.; Toke, D. A.; Mandala, S.; Martin, C. E. *J. Biol. Chem.* **1997**, *272*, 17376-17384.
- (35) Stock, S. D., *et al.* *Antimicrob. Agents Chemother.* **2000**, *44*, 1174-1180.

- (36) Powers, J.; Barlowe, C. *J. Cell Biol.* **1998**, *142*, 1209-1222.
- (37) Belden, W. J.; Barlowe, C. *J. Biol. Chem.* **1996**, *271*, 26939-26946.
- (38) Liakopoulos, D.; *et al.* *EMBO J.* **1998**, *17*, 2208-14.
- (39) Hill, W. G.; *et al.* *J. Biol. Chem.* **2007**, *282*, 37402-37411.
- (40) Hill, W. G.; An, B.; Johnson, J. P. *J. Biol. Chem.* **2002**, *277*, 33541-33544.
- (41) Bagnat, M.; *et al.* *PNAS* **2000**, *97*, 3254-3259.

VITA

Raquel Ybanez was born in Austin, Texas, on August 20, 1979; she is the daughter of Cecelia Sensing and Ismael Ybanez. She grew up in the Austin area where she successfully graduated from the Science Academy at Lyndon B. Johnson High School in 1998. Raquel then attended the University of Texas at Austin where she earned a Bachelor of Science in Chemistry with a minor in Science Education. Following graduation, she taught high school chemistry in the Austin area for four years. In August of 2007 she entered into graduate studies in the Biochemistry and Chemistry Department under the direction of Dr. Rachell E. Booth.

Permanent Address: 1716 Canon Yeomans Trail
Austin, Texas 78748

This thesis was typed by Raquel V. Ybanez

